Virologica Sinica 40 (2025) 804–811

Contents lists available at ScienceDirect

Virologica Sinica

journal homepage: www.keaipublishing.com/en/journals/virologica-sinica
www.virosin.org

Research Article

The pathogenic role and genomic characteristics of Epstein-Barr virus in vitreoretinal lymphoma

Xiaoqing Liu [a,1], Guangjie Jiang [a,1], Chianru Tan [b,1], Kun Chen [a], Zhewei Sun [a], Jiaying Du [a], Bei Wang [a], Fuqi Ai [a], Yimin Ma [a], Yueru Tian [a,*], Yong Guo [b,*], Ming Guan [a,*]

[a] Department of Laboratory Medicine, Huashan Hospital, Fudan University, Shanghai 200040, China
[b] School of Biomedical Engineering, Tsinghua University, Beijing 100084, China

ARTICLE INFO

Keywords:
Epstein-Barr virus (EBV)
Vitreoretinal lymphoma (VRL)
Genomic variants

ABSTRACT

Epstein-Barr virus (EBV) infection is well-known for its association with lymphoproliferative disorders and various lymphomas, causing significant global morbidity and mortality. EBV-positive vitreoretinal lymphoma (VRL) is exceedingly rare. As a result, the pathogenic role and genomic characteristics of EBV in VRL remain poorly understood. In this study, we employed droplet digital PCR (ddPCR) combined with EBV-specific immunofluorescence assay to detect EBV in the vitreous fluid of fifty-three VRL patients. We found that approximately 28% (15/53) of the patients were EBV positive. Analysis of clinical data showed that EBV-positive VRL patients had shorter progression-free survival (PFS) compared to EBV-negative patients ($P = 0.004$). Additionally, through integration of EBV-targeted sequencing and PCR-based deep sequencing, we found that all five VRL-derived EBV genomes formed a distinct cluster within one phylogenetic branch. Meanwhile, several non-synonymous mutations were exclusively detected in the VRL group, including S229T in latent membrane protein 1 (LMP1) and G2248R in the Epstein-Barr virus BamHI-PraL fragment 1 (BPLF1). In conclusion, our findings suggest that EBV as a risk factor associated with poor prognosis in VRL, and we provide a genome-wide view of EBV sequence variations from VRL patients. This may offer insights into the pathogenic role of EBV in VRL and could potentially assist in the diagnosis and treatment of this disease.

INTRODUCTION

Epstein-Barr virus (EBV), also known as human herpesvirus 4, is one of the most common human viruses. Transmitted through intimate contact, most infections are asymptomatic. In humans, the virus establishes latency in B lymphocytes, T lymphocytes, epithelial cells, and myocytes, and is capable of transforming lymphocytes (Liu et al., 2022). EBV infection is strongly associated with lymphoproliferative disorders and various types of lymphomas, contributing to considerable morbidity and mortality worldwide.

Vitreoretinal lymphoma (VRL) is a rare malignancy, typically classified as a diffuse large B-cell lymphoma (DLBCL) and considered a variant of primary central nervous system lymphoma (PCNSL). VRL and PCNSL are closely related: approximately 80% of VRL cases progress to PCNSL, while 20% of PCNSL cases develop VRL during the disease course. It is well-known that about 5%–10% of PCNSL patients are EBV positive (Menean et al., 2024), but the prevalence of EBV in VRL remains unclear.

In recent years, several EBV-positive VRL cases have been reported (Mittra et al., 1999; Gao et al., 2019; Ban et al., 2020; Hosseini et al., 2021; Moussa et al., 2023). Additionally, Akitaka Tsujikawa et al. found that Epstein-Barr nuclear antigen 2 (EBNA2) was positive in large-sized atypical lymphocytes in VRL (Sun et al., 2025), which represents the gold standard for diagnosing EBV-related tumors. These findings suggested that EBV may play a role in the tumorgenesis or progression of VRL. However, reports on EBV-driven VRL remain very limited due to its

* Corresponding authors.
E-mail addresses: guanming@shmu.edu.cn (M. Guan), yongguo@tsinghua.edu.cn (Y. Guo), vicky8025@126.com (Y. Tian).
[1] Xiaoqing Liu, Guangjie Jiang and Chianru Tan contributed equally to this work.

https://doi.org/10.1016/j.virs.2025.09.007
Received 22 July 2025; Accepted 24 September 2025
Available online 26 September 2025
1995-820X/© 2025 The Authors. Publishing services by Elsevier B.V. on behalf of KeAi Communications Co. Ltd. This is an open access article under the CC BY-NC-ND license (http://creativecommons.org/licenses/by-nc-nd/4.0/).

rarity, leaving its prevalence, clinical characteristics, and optimal treatment poorly identified. So, in this study, we used droplet digital PCR (ddPCR) combined with EBV-specific immunofluorescence assay to detect EBV in the vitreous fluid of VRL patients, aiming to estimate the prevalence of EBV-positive VRL. Besides, we retrospectively analyzed the association between EBV infection status and other clinical data to evaluate whether EBV-positive VRL is a distinct clinical entity.

Additionally, numerous studies have reported that natural variation in the EBV genome may play a crucial role in EBV-associated cancers. For example, single nucleotide polymorphisms (SNPs) in RPMS1, BALF2, and Epstein-Barr virus Encoded RNA 2 (EBER2) were shown to be associated with a high risk for developing nasopharyngeal carcinoma (NPC) (Xu et al., 2019). Several nonsynonymous mutations were also associated with nasal-type extranodal natural killer/T-cell lymphoma (NKTCL) (Xiong et al., 2020). Nevertheless, the genomic characteristics of EBV in VRL remain unclear. So, in this study, we employed EBV-targeted sequencing combined with PCR-based deep sequencing to analyze the genomic characteristics of EBV in the vitreous fluid of VRL patients. Phylogenetic and amino acid sequence variation analyses were performed to assess the genomic diversity of VRL-EBV genomes. We also compared the frequencies of VRL-specific EBV non-synonymous mutations among patients with VRL, PCNSL and intranodal DLBCL. Together, we presented the genetic landscape of EBV in VRL for the first time, providing insights into the pathogenic role of EBV in this disease and its potential implications for diagnosis and treatment.

RESULTS

Approximately 28% of VRL patients were EBV positive

Vitreous samples from 53 patients with VRL were included in this study. Patient demographics and clinical characteristics of VRL cases are listed in Supplementary Table S1. The median age at presentation was 60 years (range from 34 years to 76 years), and 23 (43%) were male. All patients were human immunodeficiency virus (HIV)-negative and had no known immunodeficiency. To investigate the prevalence of EBV in VRL patients, we developed a ddPCR assay to quantify EBV DNA copies in vitreous fluid. Among the 53 cases analyzed by ddPCR, 15 (approximately 28%) were identified as EBV-positive (Fig. 1A). Before clinical sample analysis, the ddPCR assay was validated using the World Health Organization (WHO) International Standard for EBV DNA, which demonstrated a linear quantification range of 10–10^6 IU/mL ($R^2 > 0.99$) (Supplementary Fig. S1). The most convincing evidence implicating EBV in tumorigenesis is demonstrated by its detection within the tumor cells. So, we conducted the EBV-specific immunofluorescence assay to identify EBV-infected cell types in the vitreous cytology specimens from

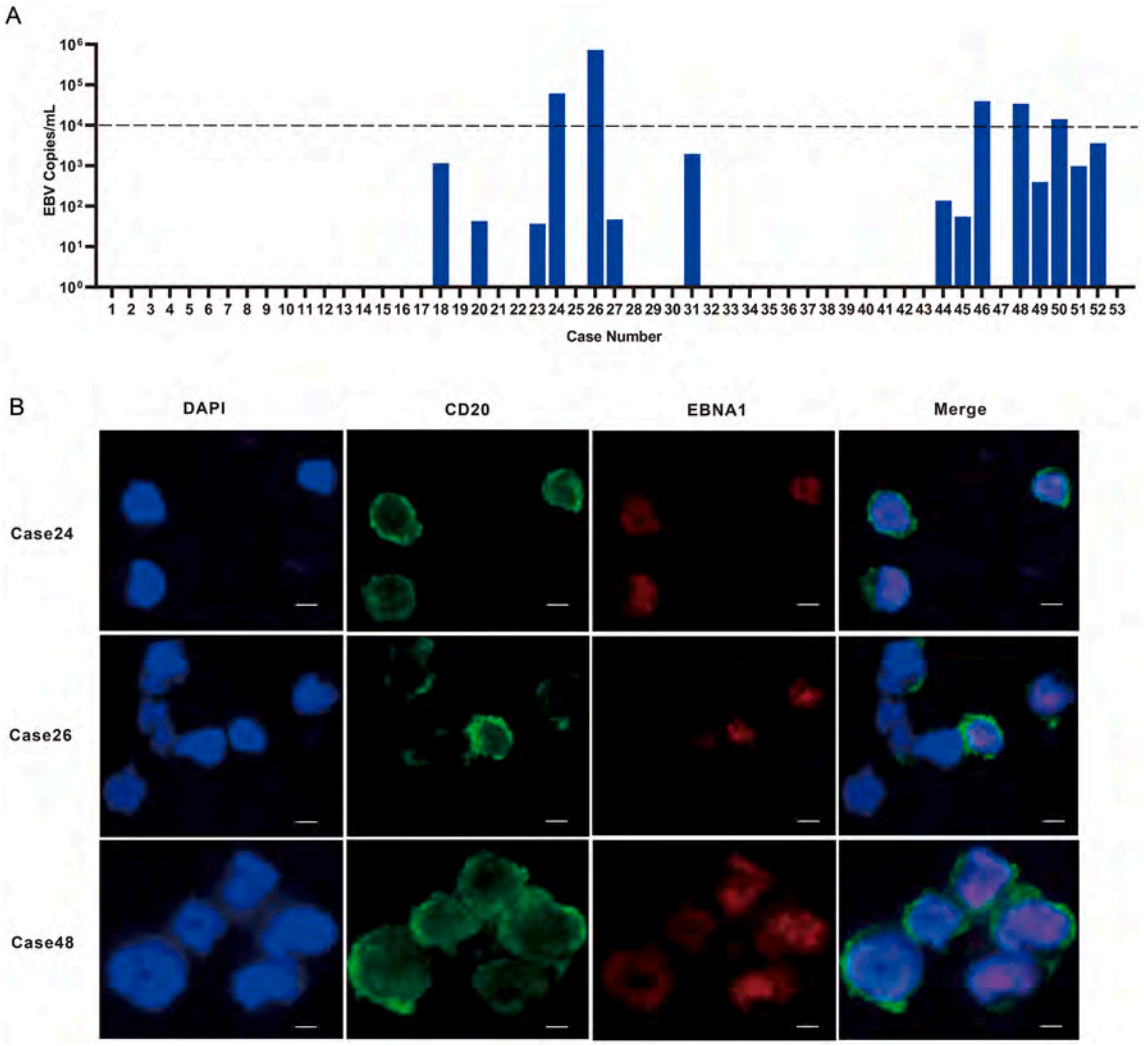

Fig. 1. EBV detection rate in vitreous fluid samples. **A** EBV DNA copies were detected in 53 vitreous fluid samples by ddPCR. **B** Immunofluorescence staining was used to detect the colocalization of EBV with CD20-positive tumor cells. Blue: DAPI indicating nuclei, Green: CD20 indicating CD20-positive tumor cells, Red: EBNA1 indicating the status of EBV infection. Numbers on the left denote case numbers. Images were acquired at 400× magnification. Scale bar: 5 μm.

cases 24, 26, 46, 48 and 50, all of which had EBV copy number exceeding 10^4 copies/ml. Unfortunately, due to the limited availability of vitreous samples, only three out of the five cases (cases 24, 26 and 48) had sufficient material for immunofluorescence assay testing. The results revealed that the EBV encoded protein Epstein-Barr nuclear antigen 1 (EBNA1) was detected in the CD20-positive malignant cells (tumor cells) in all three tested cases (Fig. 1B). This finding confirms that EBV infects tumor cells in VRL.

Patients with EBV-positive VRL showed a shorter PFS

To evaluate whether EBV-positive VRL represents a distinct clinicopathological entity compared to EBV-negative VRL, clinical data were statistically analyzed. As shown in Table 1, no significant differences were found in gender, age, serum LDH, or vitreous humor interleukin-6 (IL-6) levels between the EBV-positive and EBV-negative groups. However, vitreous interleukin-10 levels (IL-10) was significantly higher in EBV-positive group ($P = 0.006$). Additionally, consistent with EBV-positive DLBCLs, survival analysis showed that EBV positive VRL patients exhibited a significantly shortened PFS ($P = 0.004$) compared to the EBV-negative group (Fig. 2), with a median follow-up time of 24 months. In summary, these findings indicated that EBV infection is a risk factor for poor prognosis in VRL.

Table 1
Statistical analysis of clinical data.

	EBV-(n = 38)	EBV+(n = 15)	*P*-Value
Gender (M/W)	17/21	6/9	0.754
Age (M, range) (y)	61 (34–76)	58 (57–75)	0.146
LDH(U/L)	200	225 (160–399)	0.309
IL-6 (pg/mL)	336 (2.84–6937.93)	126 (6.44–679.71)	0.587
IL-8 (pg/mL)	103 (2.44–509.95)	253 (21.69–1017.81)	0.047
IL-10 (pg/mL)	273 (0.88–1963.89)	2947 (2.44–8871.46)	0.006

Note: Statistical analysis was performed using SPSS statistics software version 29 (IBM, Armonk, NY). Descriptive data were presented as the ratio, median, range, and mean. Independent sample *t*-test was used for continuous variables. Chi-square test was performed for categorical variables. A *P*-value <0.05 was considered statistically significant.

All VRL-derived EBV genomes clustered into a distinct branch

Recent advancements in deep sequencing technologies have enabled high-throughput sequencing of the EBV genome from clinical samples. These sequencing results have given rise to the hypothesis that specific EBV strains may be associated with certain EBV-related diseases. To investigate EBV genomic features in VRL, five specimens with EBV copy number exceeding 10^4 copies/mL (detected by ddPCR; see Fig. 1, including case 24, case 26, case 46, case 48 and case 50) were selected for EBV-targeted sequencing (whole-genome sequencing of EBV). The resulting sequencing reads from all five VRL-derived EBV genomes were aligned to the EBV reference sequence (GenBank accession number: NC_007605.1). Coverage rates of the five VRL-derived EBV genomes relative to the reference sequence ranged from 98.54% to 98.82%. The average sequencing depth across the target regions was 5500.78-fold, ranging from 2763.55- to 6371.64-fold. The assembled EBV genome sizes ranged from 169317 bp (VRL226) to 169791 bp (VRL0605). Detailed information on the sequencing data and differences among these five VRL-derived EBV genomes is listed in Table 2, Supplementary Tables S2 and S3.

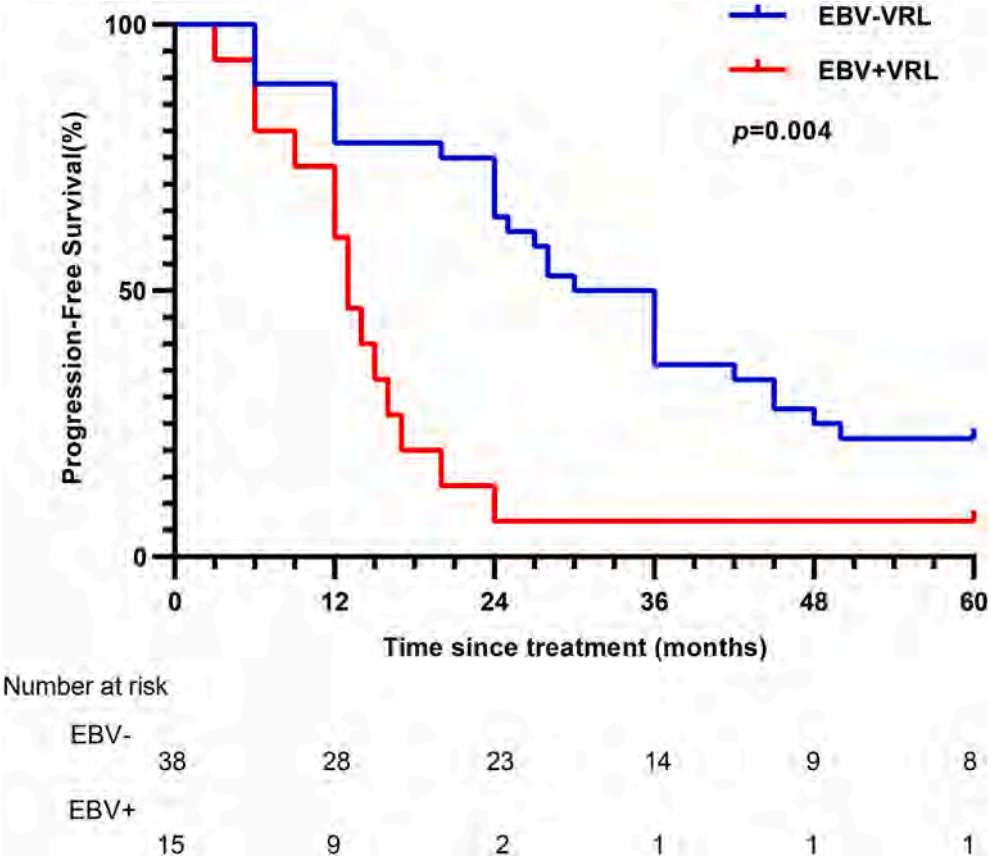

Fig. 2. Survival analysis comparing EBV-positive and EBV-negative VRL patients. EBV positivity was an independent indicator of adverse progression-free survival. Univariate Kaplan-Meier estimations were performed with the log-rank test. EBV-, EBV negative; EBV+, EBV positive; PFS, progression-free survival. The table at the bottom shows the number of at-risk patients at key time points.

Table 2
Summary of EBV-targeted sequencing data.

Sample	No. of reads		Mapped bases (bp)	Coverage (%)	Sequencing depth(X)	Length (bp)	No.of variations		
	Raw	Mapped					Substitutions	Insertions	Deletions
VRL226	64681262	3165613	474841950	98.54	2763.55	169317	773	11	20
VRL1111	132029262	7295388	1094308200	98.68	6368.81	169555	784	13	18
VRL1421	127463736	6524200	978630000	98.70	5695.57	169593	852	14	18
VRL1949	140501264	7298625	1094793750	98.56	6371.64	169347	795	10	19
VRL0605	136617234	7221535	1083230250	98.82	6304.34	169791	791	6	19

Note:Raw reads refers to the total number of sequencing reads, and Mapped reads/bases refers to the number of reads/bases successfully aligned to the reference genome(GenBank accession number: NC_007605.1). Coverage is the fraction of the EBV reference sequence spanned by mapped reads. Sequencing depth was calculated using the following formula: Total number of base pairs mapped to the reference genome/Total length of the reference genome numbers of variations refer to the numbers of substitutions, insertions and deletions in every sample.

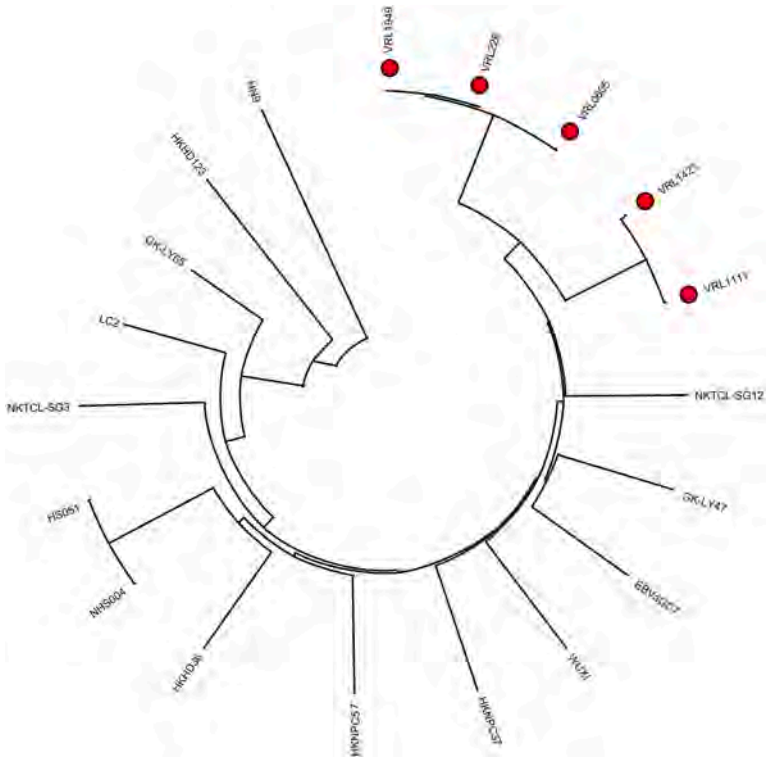

Fig. 3. Phylogenetic analysis of whole EBV genomic sequences. The phylogenetic tree includes five VRL-derived EBV genomes assembled in this study and other published EBV strains from various regions of China. Phylogenetic analysis was conducted using the neighbor-joining algorithm based on the full-length EBV genomes using MEGA12, with the bootstrap value set at 1000. VRL226, VRL1111, VRL1421, VRL1949, and VRL0605 correspond to Case 24, Case 26, Case 46, Case 48, and Case 50 in Fig. 1, respectively.

Phylogenetic trees were constructed using the complete genome sequences of the five VRL-derived EBV assembled in this study, along with other previously published EBV genomes. The resulting phylogeny revealed that all VRL-derived EBV genomes formed a distinct clade, clearly separate from EBV strains isolated from multiple regions across China (Fig. 3), suggesting that VRL may possess unique EBV genomic features.

VRL-specific EBV genomic variants were identified in VRL patients

A comparative variation analysis were performed among the five VRL-derived EBV genomes using the reference EBV sequence (GenBank accession number: NC_007605.1). On average, 799 EBV single-nucleotide variations (SNVs) per sample were identified (Supplementary Table S2), with the highest incidences of variations located within the 80–100 kb and 160–170 kb regions (Fig. 4A). The genes encoding latent membrane protein 1 (LMP1), Epstein-Barr nuclear antigen 3C (EBNA3C), Epstein-Barr virus BamHI-PraL fragment 1(BPLF1) and EBNA1 showed the highest frequencies of nonsynonymous mutations (Fig. 4B). To determine whether these nonsynonymous mutations are specific to VRL, we employed PCR-based deep sequencing to evaluate the prevalence of 60 nonsynonymous mutations in vitreous fluid samples from VRL patients. These results were compared with those from EBV-positive intranodal DLBCL (lymph node specimens) and PCNSL (brain tissue specimens). As shown in Fig. 4C, the LMP1 variant G331R and the BPLF1 variant S2696T were detected in nearly all samples, consistent with previous reports in other EBV-associated cancers (Palser

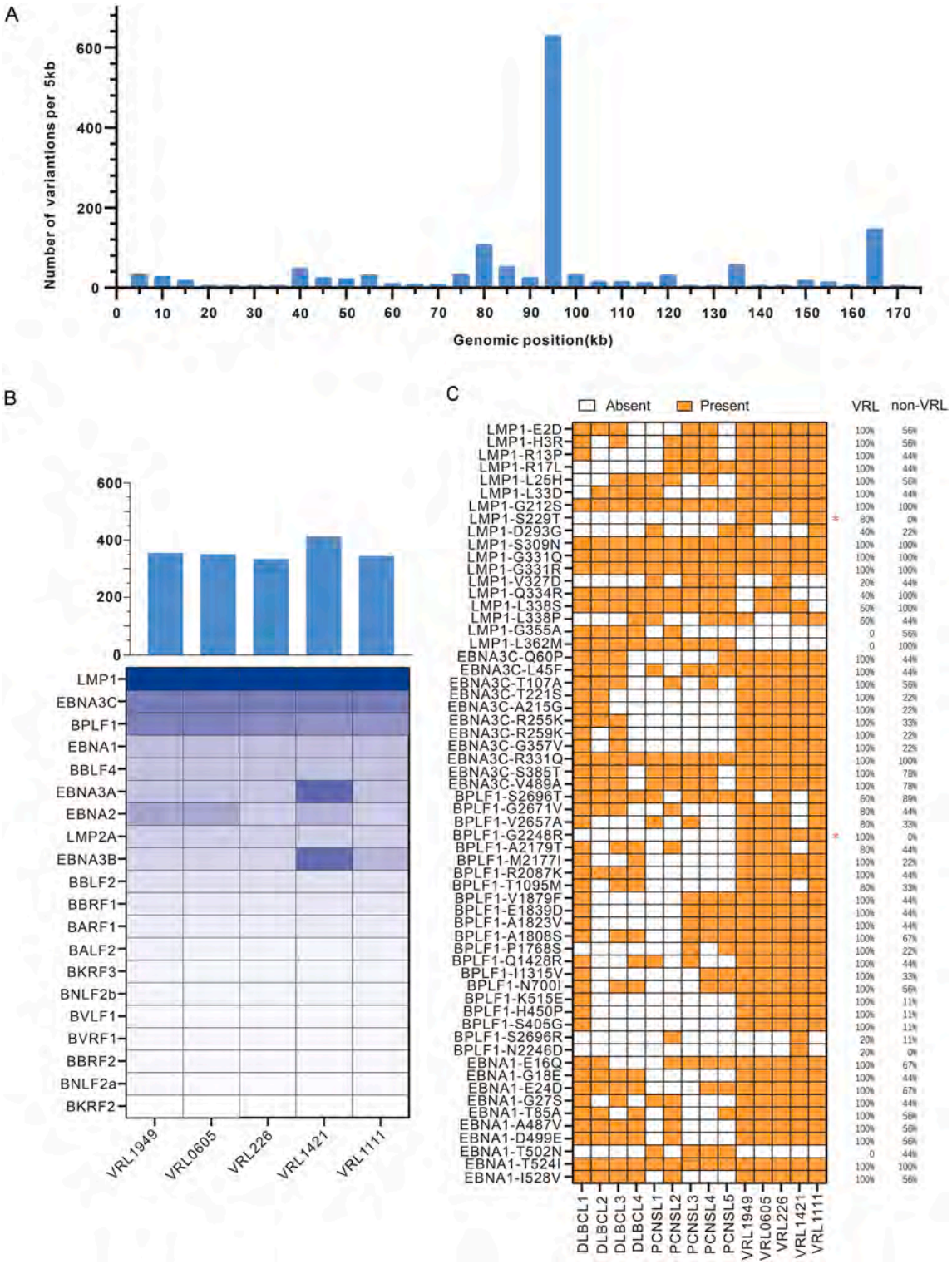

Fig. 4. Genetic variation analysis of VRL-derived EBV genomes. **A** Genome-wide distribution of single-nucleotide variations (SNVs) in the five VRL-derived EBV genomes. **B** The number of all nonsynonymous mutations identified in the five VRL-derived EBV genomes. Top: The bar chart represents the total nonsynonymous mutations of each sample. Bottom: The heatmap represents the nonsynonymous mutation numbers of every gene. Each column represents a sample and each row represents a specific gene. The color gradient from white to blue indicates an increasing mutation frequency. **C** Prevalence of 60 non-synonymous mutations in the vitreous fluid from EBV positive VRL patients, compared with specimens from EBV positive non-VRL patients (including intranodal DLBCL and PCNSL). White cells indicate no mutation detected, orange cells indicate a mutation (VAF >0.50). Mutation frequencies in non-VRL and VRL groups are listed on the right. Variants potentially associated with VRL are marked with asterisks. DLBCL: intranodal diffuse large B-cell lymphoma; PCNSL: primary central nervous system lymphoma; VRL: vitreoretinal lymphoma.

et al., 2015). However, new mutation hotspots, such as S229T in LMP1 and G2248R in BPLF1, were observed exclusively in the VRL group. All detected mutations per case are provided in Supplementary Table S4. Together, these findings indicate the presence of VRL-specific EBV genomic variants.

DISCUSSION

VRL is a rare B-cell intraocular neoplasia characterized by a poor long-term prognosis and a lack of effective therapies. Due to the lack of worldwide consensus about diagnosis, therapy, and follow-up timing, VRL represents one of the most challenging ocular disorders (Menean et al., 2024). Two main theories have been proposed regarding the etiology of VRL: the infectious theory and the hematological spread theory. According to the infectious theory, infections with EBV or HIV, especially in immunocompromised patients, recall lymphoid cells, leading to neoplastic transformation and the development of lymphoid malignancy in the eye and/or central nervous system (CNS) subsequently (Hosseini et al., 2021).

In this study, to investigate the relationship between EBV infection status and VRL, we established two methods to detect EBV in vitreous specimens: ddPCR for quantifying EBV DNA, and EBV-specific immunofluorescence assay for precise localization of EBV within tumor cells. Consistent with its prevalence in PCNSL, EBV was predominantly detected in CD20 positive tumor cells. However, the prevalence of EBV in VRL was higher than in PCNSL, which may be attributable to the high sensitivity of ddPCR. Notably, our VRL cases were mostly secondary VRL (from PCNSL), implying that some patients may have already received treatment. Some treatment, such as methotrexate intrathecal or intravenous injection, can effectively reduce the EBV-DNA load (Yin et al., 2022). When patients were stratified by treatment status (with 11 cases excluded due to unavailable treatment information), the EBV positivity rate was significantly higher in the untreated group than in the treated group [48% (13/27) vs. 13% (2/15), $P = 0.024$)]. Besides, most vitreous samples were diluted with normal saline, which may further reduce the viral detection rate. These confounding factors suggest that the actual prevalence of EBV in VRL may be higher than observed. Furthermore, analysis of clinical data revealed that patients in the EBV-positive group had shorter PFS than those in the EBV-negative group. This finding emphasizes the importance of assessing EBV infection status during the diagnosis of VRL, as this subtype requires appropriate therapeutic strategies tailored to its highly aggressive.

Through phylogenetic and amino acid sequence variation analyses of VRL-derived EBV genomes, we found that all VRL-EBV genomes clustered within one branch, and a few EBV genomic variations, such as the LMP1 variant S229T and the BPLF1 variant G2248R, were exclusively detected in the VRL group. This finding contrasts with previous reports indicating that PCNSL and VRL have similar host gene mutation profiles (Bonzheim et al., 2015; Lee et al., 2020). To date, no studies have yet addressed whether these mutations hold biological significance. So, further studies are needed to clarify the relationship between these mutation sites and the development of VRL, as well as their potential utility as diagnostic biomarkers for VRL. Besides, through VAF analysis, we found that the genomic heterogeneity of EBV in the PCNSL group is higher than that in the VRL group (Supplementary Fig. S2), consistent with other studies reporting that PCNSL is a highly heterogeneous tumor type (Hernández-Verdin et al., 2023). These data suggest that EBV may undergo an evolutionary process as it enters the central nervous system. However, paired intraocular and CNS samples from patients with secondary PCNSL (following VRL) should be included to validate this hypothesis.

Limitations of this study include the cohort size, which reflects the rarity of EBV-positive VRL and the lack of tissue availability. This limits the generalizability of our genomic findings. Larger cohorts of paired VRL liquid biopsies and PCNSL tumor tissues from the same patient will be needed to analyze the evolution process of EBV between eyes and CNS. Further, because of the limitations in short-read sequencing and the proximity of some genes to repeat regions of the genome, parts of the EBV genome could not be evaluated. Short-read sequencing also limits our ability to determine if allele frequency differences are caused by multiple strains or SNPs occurring secondary to rapid viral replication within the tumor. Thus, future studies should integrate long-read sequencing to resolve viral structures.

CONCLUSIONS

In summary, our study provides evidence supporting an association between EBV infection and VRL, and suggests that EBV variation testing may serve as a discriminating marker to differentiate VRL from other types of DLBCLs. Future studies should expand to multicenter cohorts with paired liquid/tissue biopsies, which will be instrumental in developing appropriate diagnostic and therapeutic strategies. Moreover, whether the unique EBV variants actively drive the development of VRL or simply adapted to the niche of VRL as bystanders awaits further investigations.

MATERIALS AND METHODS

VRL patients and clinical data

Fifty-three patients suspected of VRL underwent diagnostic vitrectomy at Huashan Hospital, Fudan University, from 2017 to 2024. The diagnostic criteria for VRL was the same as our previous study (Chen et al., 2024). At the time of initial diagnosis and before each treatment, Positron Emission Tomography-Computed Tomography (PET-CT), brain and spinal magnetic resonance imaging (MRI), Bone Marrow (BM), and ocular evaluation were performed. Then, all vitreous specimens were examined by cytology, immunocytochemistry for B-cell markers, and flow cytometry for IL-10/IL-6, and ddPCR for EBV DNA. All included patients were HIV-negative and had no other ocular or neurological diseases at diagnosis. The median follow-up time of this study was 24 months, with all patients followed up every 3 months. This study was approved by the Institutional Review Board of Huashan Hospital, Fudan University (Approval No. KY2014-163). Written informed consent was obtained from each participant. All the examinations were performed according to the Declaration of Helsinki.

DNA extraction

Cell-free DNA (cfDNA) was extracted from 1 mL of vitreous fluids using the Nucleic Acid Extraction Kit cfDNA-B1 (TargetingOne, Beijing, China, 11014), according to the manufacturer's instructions. The cfDNA was eluted in a final volume of 100 μL. Tumor DNA was extracted from formalin-fixed, paraffin-embedded (FFPE) tissue using the TIANamp FFPE DNA Kit (Tiangen, Beijing, China, DP340).

Detection of EBV using droplet digital PCR (ddPCR)

Absolute quantification of EBV viral load was performed using the EBV Nucleic Acid Detection Kit (Digital PCR Method) (TargetingOne, Beijing, China; Cat. No. 13595), which targets the EBNA1 and BamHI-W regions of the EBV genome, and the TD-2 Droplet Digital PCR System (TargetingOne, Beijing, China), following the manufacturer's instructions. Briefly, a 30 μL reaction mixture was prepared for each sample, comprising 7.5 μL of PCR Mix A, 7.5 μL of primer/probe mix (PCR Mix B), and 15 μL of DNA template. The 30 μL reaction mixture and 180 μL of droplet generation oil were loaded into a droplet generation chip. Droplets were generated using the Drop Maker M1 (TargetingOne, Beijing, China) to form a water-in-oil emulsion. Thermal cycling was performed under the following conditions: initial denaturation at 95 °C for 30 s, followed by 40 cycles of denaturation at 94 °C for 10 s and annealing at 57 °C for 30 s, and a final hold at 12 °C. After amplification,

the PCR tube containing the droplets was connected to a droplet detection chip and placed in the Chip Reader R2 (TargetingOne, Beijing, China) to detect fluorescent signals. Data were analyzed using ChipReaderR2 software (TargetingOne, Beijing, China) based on Poisson distribution to determine the absolute copy numbers of each target.

The EBV viral load (copies/mL) in vitreous samples was calculated as follows: EBV EBV viral load (copies/mL) = (total detected EBV copies/total template volume) × (elution volume/extracted vitreous sample volume). Quantitative performance was validated using quadruplicate measurements of serial dilutions (10–10^6 IU/mL) of the WHO International Standard for EBV DNA (NIBSC 09/260). Conversion factors were established by linear regression (Supplementary Fig. S1) comparing ddPCR copies/mL to reference IU/mL values: for EBNA1: 1 copy = 0.39 IU; for BamHI-W: 1 copy = 0.07 IU.

Immunofluorescence assay

Vitreous fluid biopsies were pre-fixed with PreservCyt Solution (HOLOGIC) (Wang et al., 2021) immediately after collection, then centrifuged onto 0.1% fish skin gelatin (Sigma, G-7765) pre-treated slides using Cytospin (Sayk-Cytospin, Huashan hospital). Subsequently, immunofluorescence assays were performed. Briefly, cells were permeabilized in PBS containing 0.2% fish skin gelatin and 0.02% Triton X-100 (TBST) for 5 min, then incubated with primary antibodies against EBNA1 (Santa Crus, sc-81581) and CD20 (Servicebio, GB155721) for 1 h at room temperature. After three washes with TBST, cells were incubated with Alexa Fluor-conjugated secondary antibodies for 1 h at room temperature. Finally, Cell nuclei were counterstained with DAPI. Slides were visualized with a Leica SP8 confocal microscope.

Library preparation and sequencing for analyzing EBV genome variations

Fragmented DNA templates were generated using ultrasonic crusher. A unique barcode was added to each DNA sample using the KAPA HyperPrep Kit from Roche. Samples were pooled based on EBV load and prepared according to the xGen hybridization capture of DNA libraries for the NGS sequencing enrichment protocol. The capture probes were synthesized as custom hybridization capture panels designed for the EBV reference genome (GenBank accession number: NC_007605.1) with 10 × coverage. EBV capture samples were sequenced using a NovaSeq6000 (Illumina). Sequence reads were adapter-trimmed using an in-house program. Then, the processed reads were aligned to NC_007605.1 using NovoAlign (NovoCraft, http://novocraft.com) with default parameters and a '-r Random' option. Variants were detected using VarScan2 and annotated using ANNOVAR with NC_007605.1 information.

PCR-based deep sequencing

VRL-derived EBV nonsynonymous mutations were validated in tumor samples from VRL, PCNSL and systemic DLBCL patients using PCR-based deep sequencing. Briefly, specific primers (Supplementary Table S5) equipped with adapter sequences at the 5′-terminal were used for PCR amplification of the EBV genes. Next, PCR products were sequenced on an Illumina NovaSeq6000 platform with 2 × 150 bp end reads, about 100,000 reads per sample was obtained. After filtering the raw data, the obtained reads were aligned to the reference EBV genome to detect SNPs using MAFFT.

Phylogenetic analysis

Molecular Evolutionary Genetics Analysis (MEGA) software was used to align five VRL-derived EBV subtypes with published EBV genomes, including the reference genome (NC_007605.1), EBVaGC7 (KT273947.1), HN9 (AB850659.1), HKNPC37 (MH590548.1), HKNPC57 (MH590568.1), GK-LY47 (MG298840.1), GK-LY65 (MG298841.1), NKTCL-SG3 (MH144214.1), NKTCL-SG12 (MH144223.1), HKHD36 (MH590405.1), HKHD123 (MH590492.1), NHS004 (MK540302.1), HS051 (MK540296.1), LC2 (KT823507.1) and WUXI (PQ541390.1). Phylogenetic analysis was conducted using the neighbor-joining algorithm based on multiple sequence alignments of all EBV genomes.

Statistical analysis

Statistical analyses were performed using SPSS statistics software version 29 (IBM, Armonk, NY). Descriptive data are presented as ratios, medians, ranges, and means. Independent samples *t*-tests were used for continuous variables. Chi-square test was performed for categorical variables. A *P*-value <0.05 was considered statistically significant.

DATA AVAILABILITY

The raw sequence data reported in this paper have been deposited in the ScienceDB (https://doi.org/10.57760/sciencedb.27467) and further inquiries can be directed to the corresponding authors.

ETHICS STATEMENT

This study was performed in compliance with an institutional review board protocol at Huashan Hospital (KY2014-163). Written informed consent was obtained from each participant.

AUTHOR CONTRIBUTIONS

Liu Xiaoqing: conceptualization, data curation, investigation, methodology, software, writing-original draft. Jiang Guangjie: data curation, methodology, resources, writing-original draft. Tan Chianru: methodology, writing-original draft. Chen Kun: investigation, resources, supervision. Sun Zhewei: data curation, validation. Du Jiaying: data curation, validation. Wang Bei: data curation, validation. Ai Fuqi: investigation, project administration. Ma Yimin: formal analysis. Tian Yueru: investigation, supervision, visualization. Guo Yong: methodology, supervision. Guan Ming: funding acquisition, supervision, writing-reviewing and editing.

CONFLICT OF INTEREST

The authors declare no conflict of interest.

ACKNOWLEDGEMENTS

This work was supported by the Basic Research Youth Talent Development Program of Huashan Hospital, Fudan University (2024JC030).

APPENDIX A. SUPPLEMENTARY DATA

Supplementary data to this article can be found online at https://doi.org/10.1016/j.virs.2025.09.007.

REFERENCES

Ban, Y., Okamoto, M., Ogata, N., 2020. Case of primary intraocular lymphoproliferative disorder caused by Epstein-Barr Virus. BMC Ophthalmol. 20, 306.

Bonzheim, I., Giese, S., Deuter, C., Süsskind, D., Zierhut, M., Waizel, M., Szurman, P., Federmann, B., Schmidt, J., Quintanilla-Martinez, L., Coupland, S.E., Bartz-Schmidt, K.U., Fend, F., 2015. High frequency of MYD88 mutations in vitreoretinal B-cell lymphoma: a valuable tool to improve diagnostic yield of vitreous aspirates. Blood 126, 76–79.

Chen, K., Qin, H., Li, X., Zhou, X., Ma, J., Guan, M., 2024. Diagnostic potential of vitreoretinal lymphoma by detection of gene mutations with NGS in 25 Chinese patients. Clin. Chim. Acta 561, 119827.

Gao, S., Zhou, Y., Jin, X., Lin, Z., Zhong, Y., Shen, X., 2019. Primary vitreoretinal natural killer/T-cell lymphoma with breast involvement: a case report and review of the literature. Surv. Ophthalmol. 64, 225–232.
Hernández-Verdin, I., Kirasic, E., Wienand, K., Mokhtari, K., Eimer, S., Loiseau, H., Rousseau, A., Paillassa, J., Ahle, G., Lerintiu, F., et al., 2023. Molecular and clinical diversity in primary central nervous system lymphoma. Ann. Oncol. 34, 186–199.
Hosseini, S.M., Abrishami, M., Barashki, E., Zamani, G., 2021. Primary intraocular lymphoma in a patient with bilateral Epstein-Barr virus panuveitis. Case Rep Ophthalmol Med 2021, 9496173.
Lee, J., Kim, B., Lee, H., Park, H., Ho Byeon, S., Choi, J.R., Lee, S.C., Lee, S.T., Lee, C.S., 2020. Whole exome sequencing identifies mutational signatures of vitreoretinal lymphoma. Haematologica 105, e458–e460.
Liu, M., Wang, X., Zhang, L., Feng, G., Zeng, Y., Wang, R., Xie, Z., 2022. Epidemiological characteristics and disease burden of infectious mononucleosis in hospitalized children in China: a nationwide retrospective study. Virol. Sin. 37, 637–645.
Menean, M., Giuffrè, C., Cicinelli, M.V., Marchese, A., Modorati, G., Bandello, F., Miserocchi, E., 2024. A comprehensive overview of diagnosis, imaging and treatment of vitreoretinal lymphoma. Eur. J. Ophthalmol. 34, 931–940.
Mittra, R.A., Pulido, J.S., Hanson, G.A., Kajdacsy-Balla, A., Brummitt, C.F., 1999. Primary ocular Epstein-Barr virus-associated non-Hodgkin's lymphoma in a patient with AIDS: a clinicopathologic report. Retina 19, 45–50.
Moussa, K., Gonzales, J.A., Shantha, J., Acharya, N.R., Doan, T., 2023. Prevalence of Epstein-Barr virus in patients with intraocular inflammation. Ocul. Immunol. Inflamm. 31, 978–980.
Palser, A.L., Grayson, N.E., White, R.E., Corton, C., Correia, S., Ba Abdullah, M.M., Watson, S.J., Cotten, M., Arrand, J.R., Murray, P.G., Allday, M.J., Rickinson, A.B., Young, L.S., Farrell, P.J., Kellam, P., 2015. Genome diversity of Epstein-Barr virus from multiple tumor types and normal infection. J. Virol. 89, 5222–5237.
Sun, C., Muraoka, Y., Ishihara, K., Morooka, S., Akada, M., Hata, M., Tsujikawa, A., 2025. A case OF epstein-barr virus-associated primary vitreoretinal lymphoma in an immunosuppressed patient. Retin. Cases Brief Rep. 19, 23–27.
Wang, M.M., Tan, W.J., Lim, T.S., Chan, A.S.Y., 2021. PreservCyt is an optimal fixative that permits cytologic and molecular analyses of vitreoretinal lymphoma biopsies. Ocul. Immunol. Inflamm. 29, 430–439.
Xiong, J., Cui, B.W., Wang, N., Dai, Y.T., Zhang, H., Wang, C.F., Zhong, H.J., Cheng, S., Ou-Yang, B.S., Hu, Y., et al., 2020. Genomic and transcriptomic characterization of natural killer T cell lymphoma. Cancer Cell 37, 403–419.e406.
Xu, M., Yao, Y., Chen, H., Zhang, S., Cao, S.M., Zhang, Z., Luo, B., Liu, Z., Li, Z., Xiang, T., et al., 2019. Genome sequencing analysis identifies Epstein-Barr virus subtypes associated with high risk of nasopharyngeal carcinoma. Nat. Genet. 51, 1131–1136.
Yin, Q., Wang, J., Wang, Z., 2022. Epstein-Barr virus central nervous system involvement in Epstein-Barr virus-associated hemophagocytic lymphohistiocytosis. Ann. Hematol. 101, 2471–2476.